

## Synthesis and Characterization of Hydrogen-Bonded Assemblies of $W_6S_8L_6$ Clusters

Catherine M. Oertel, Ryan D. Sweeder,<sup>†</sup> Sonal Patel,<sup>‡</sup> Craig M. Downie,<sup>§</sup> and Francis J. DiSalvo\*

Department of Chemistry and Chemical Biology, Cornell University, Ithaca, New York 14853

Received September 13, 2004

Ligand-exchange reactions involving octahedral  $W_6S_8$  clusters and a family of pyridine-based ligands (isonicotinic acid, isonicotinamide, 4-hydroxypyridine, 4-aminopyridine, 4-pyridineacetamide) have been explored with the goal of preparing compounds that crystallize in hydrogen-bonded arrays. Two new compounds,  $W_6S_8(4\text{-pyridineacetamide})_6 \cdot \text{DMF} \cdot 4\text{-pyridineacetamide}$  (**1**) and  $W_6S_8(4\text{-aminopyridine})_6 \cdot 4\text{DMF}$  (**2**), were isolated and characterized by single-crystal X-ray diffraction. Both compounds crystallize in the  $P2_1/c$  space group with  $a = 16.461(1)$ ,  $b = 33.08(2)$ ,  $c = 13.165(10)$  Å,  $\beta = 103.270(15)^\circ$  for **1** and  $a = 13.8988(5)$ ,  $b = 13.2791(5)$ ,  $c = 15.6293(6)$  Å,  $\beta = 108.5410(10)^\circ$  for **2**. Each compound was further characterized by  $^1\text{H}$  NMR spectroscopy, elemental (CHN) analysis, and thermogravimetric analysis. Examination of the structures shows that **1** forms a three-dimensional hydrogen-bonded network in which each 4-pyridineacetamide ligand interacts with ligands on neighboring clusters or with the free ligand of crystallization. This is the first hydrogen-bonded network formed from  $W_6S_8$  clusters. In **2**, the amino groups act as hydrogen-bond donors toward DMF molecules of crystallization, but an extended array is not formed. In addition, the binding strengths of these pyridine-based ligands to the  $W_6S_8$  cluster were studied through quantitative  $^1\text{H}$  NMR studies of ligand-exchange reactions. A qualitative relationship was found between ligand binding strengths and Hammett substituent constants for this group of ligands.

### Introduction

Octahedral group 6 metal clusters of the form  $M_6Q_8L_6$  ( $M = \text{Mo, W}$ ;  $Q = \text{S, Se, Te}$ ;  $L = \text{Lewis-basic organic ligand}$ ) have been the subject of much interest over the last several decades. Since these soluble, molecular clusters became accessible due to the work of Saito<sup>1,2</sup> and McCarley,<sup>3,4</sup> research has been directed toward understanding their synthesis,<sup>5,6</sup> electrochemistry,<sup>7,8</sup> and ligand-exchange chemistry.<sup>9,10</sup> One reason for the great interest in these cluster

compounds has been their structural relationship with the fascinating molybdenum-based Chevrel phases, which are well-known for their superconductivity,<sup>11,12</sup> fast-ion conductivity,<sup>13,14</sup> and catalytic properties.<sup>15,16</sup> We have been interested in preparing organic–inorganic network materials from  $W_6S_8$  building blocks since theoretical work has shown that such materials might also be expected to have interesting electronic and/or magnetic properties.<sup>17,18</sup> While networks

\* Author to whom correspondence should be addressed. E-mail: fjd3@cornell.edu.

<sup>†</sup> Current address: Lyman Briggs School, Michigan State University, East Lansing, MI 48825-1107.

<sup>‡</sup> NSF REU student from Barnard College, New York, NY.

<sup>§</sup> Current address: Diamond Innovations, Worthington, OH 43085.

- (1) Saito, T.; Yamamoto, N.; Yamagata, T.; Imoto, H. *J. Am. Chem. Soc.* **1988**, *110*, 1646–1647.
- (2) Saito, T.; Yoshikawa, A.; Yamagata, T. *Inorg. Chem.* **1989**, *28*, 3588–3592.
- (3) Hilsenbeck, S. J.; Young, V. G.; McCarley, R. E. *Inorg. Chem.* **1994**, *33*, 1822–1832.
- (4) Zhang, X.; McCarley, R. E. *Inorg. Chem.* **1995**, *34*, 2678–2683.
- (5) Venkataraman, D.; Rayburn, L. L.; Hill, L. I.; Jin, S.; Malik, A.-S.; Turneau, K. J.; DiSalvo, F. J. *Inorg. Chem.* **1999**, *38*, 828–830.
- (6) Jin, S.; Popp, F.; Boettcher, S. W.; Yuan, M.; Oertel, C. M.; DiSalvo, F. J. *J. Chem. Soc., Dalton Trans.* **2002**, 3096–3100.

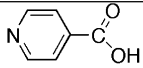
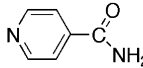
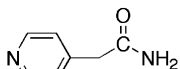
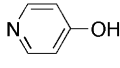
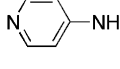
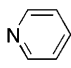
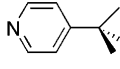
- (7) Saito, T.; Yamamoto, N.; Nagase, T.; Tsuboi, T.; Kobayashi, K.; Yamagata, T.; Imoto, H.; Unoura, K. *Inorg. Chem.* **1990**, *29*, 764–770.
- (8) Hill, L. I.; Jin, S.; Zhou, R.; Venkataraman, D.; DiSalvo, F. J. *Inorg. Chem.* **2001**, *40*, 2660–2665.
- (9) Jin, S.; Venkataraman, D.; DiSalvo, F. J. *Inorg. Chem.* **2000**, *39*, 2747–2757.
- (10) Jin, S.; Zhou, R.; Scheuer, E. M.; Adamchuk, J.; Rayburn, L. L.; DiSalvo, F. J. *Inorg. Chem.* **2001**, *40*, 2666–2674.
- (11) Chevrel, R.; Sergent, M.; Prigent, J. *J. Solid State Chem.* **1971**, *3*, 515–519.
- (12) Chevrel, R.; Hirrien, M.; Sergent, M. *Polyhedron* **1986**, *5*, 87–94.
- (13) Mulhern, P. J.; Haering, R. R. *Can. J. Phys.* **1984**, *62*, 527–531.
- (14) Aurbach, D.; Lu, Z.; Schechter, A.; Gofer, Y.; Gizbar, H.; Turgeman, R.; Cohen, Y.; Moshkovich, M.; Levi, E. *Nature* **2000**, *407*, 724–727.
- (15) McCarty, K. F.; Anderegg, J. W.; Schrader, G. L. *J. Catal.* **1985**, *93*, 375–387.
- (16) Thompson, R. K.; Hilsenbeck, S. J.; Paskach, T. J.; McCarley, R. E.; Schrader, G. L. *J. Mol. Catal. A: Chem.* **2000**, *161*, 75–87.

of  $W_6S_8(CN)_6^{6-}$  clusters mediated by single transition metals have been prepared,<sup>19</sup> these are currently the only known examples of crystalline  $W_6S_8$ -based networks, and new approaches are needed to construct cluster-organic materials.

One means by which crystalline arrays of  $W_6S_8$  clusters may be prepared is use of Lewis-basic ligands that can coordinate to the cluster and also contain functional groups that can participate in intermolecular hydrogen-bonding interactions with ligands on neighboring clusters. Hydrogen bonding has been widely used in building supramolecular structures based on organic molecules<sup>20–22</sup> and, more recently, on hybrid inorganic–organic systems.<sup>23–26</sup> Hydrogen-bonded networks of transition metal complexes have been synthesized,<sup>27</sup> producing compounds with high porosity<sup>27h</sup> and leading to speculation that compounds with interesting electronic and optical properties may be accessible through this approach.<sup>27c</sup> Some recent work has also involved building hydrogen-bonded arrays of octahedral metal clusters. Two hydrogen-bonded networks of  $Mo_6Cl_8^{4+}$  clusters have been assembled,<sup>28</sup> as have one- and two-dimensional arrays based on the related group 7  $Re_6Se_8^{2+}$  clusters.<sup>29,30</sup> However, this method has never been applied to uncharged, electrically neutral clusters such as  $W_6S_8$ .

Pyridine-based ligands have often been used in constructing hydrogen-bonded networks of transition metals because of the rigid directionality that they impart and because they are able to bind to a variety of metal centers.<sup>27c</sup> However, the bulkiness of these ligands makes it difficult to achieve octahedral coordination around single metal centers, limiting their utility in constructing three-dimensional networks. Pyridine and 4-*tert*-butylpyridine have previously been used

**Table 1.** Properties of Pyridine-Based Ligands

ligand	structure	pK <sub>a</sub> <sup>a</sup>	σ <sup>b</sup>
isonicotinic acid		1.75 <sup>c</sup>	0.44
isonicotinamide		3.55 <sup>d</sup>	0.30
4-pyridineacetamide		5.08 <sup>e</sup>	0.07
4-hydroxypyridine		4.82 <sup>f</sup>	-0.92
4-aminopyridine		9.11 <sup>g</sup>	-1.31
pyridine		5.25 <sup>h</sup>	0.00
4- <i>tert</i> -butylpyridine		6.0 <sup>h</sup>	-0.26

<sup>a</sup> For loss of a proton from the conjugate pyridinium cation. <sup>b</sup> Hammett substituent constant. <sup>c</sup> From ref 32. <sup>d</sup> From ref 33. <sup>e</sup> From ref 34. <sup>f</sup> From ref 35. <sup>g</sup> From ref 36. <sup>h</sup> From ref 10.

as ligands for  $W_6S_8$  clusters,<sup>31</sup> and the considerable size of the clusters makes full octahedral coordination possible. Use of pyridine-based ligands bearing hydrogen-bonding substituents may not only be a new means of assembling arrays of  $W_6S_8$  clusters but may also expand the repertoire of hydrogen-bonding motifs seen in transition metal networks.

A group of pyridine-based ligands with moieties capable of acting as hydrogen-bond donors and/or acceptors was selected for study. These ligands are shown in Table 1, along with the pK<sub>a</sub>'s of their conjugate pyridinium cations and their Hammett substituent constants. The previously studied ligands 4-*tert*-butylpyridine and pyridine have been included as points of reference. In addition to being of interest for their potential use in building cluster networks, these ligands are ideal for correlation studies of binding abilities because they differ only in the identity of their ring substituents. Although pK<sub>a</sub> is sometimes a good indicator of how effectively a ligand will coordinate to the  $W_6S_8$  cluster, it has significant limitations in predicting these binding abilities.<sup>10</sup> Hammett parameters have been shown to be useful in correlating the abilities of ligands to bind to single metal centers. Stability constants of complexes of Ag<sup>+</sup> ions and pyridine-based ligands have been correlated with Hammett parameters,<sup>37</sup> as have strengths of coordination of pyridine-

- (17) Hughbanks, T.; Hoffmann, R. *J. Am. Chem. Soc.* **1983**, *105*, 1150–1162.
- (18) Malik, A.-S. Ph.D. Dissertation, Cornell University, 1998.
- (19) Jin, S.; DiSalvo, F. *J. Chem. Mater.* **2002**, *14*, 3448–3457.
- (20) Lehn, J.-M. *Supramolecular Chemistry: Concepts and Perspectives*; VCH: Weinheim, Germany, 1995.
- (21) Desiraju, G. R. *Crystal Engineering: The Design of Organic Solids*; Elsevier: New York, 1989.
- (22) Etter, M. C. *Acc. Chem. Res.* **1990**, *23*, 120–126.
- (23) Burrows, A. D.; Chan, C.-W.; Chowdhry, M. M.; McGrady, J. E.; Mingos, D. M. P. *Chem. Soc. Rev.* **1995**, 329–339.
- (24) Burrows, A. D.; Mingos, D. M. P.; White, A. J. P.; Williams, D. J. *J. Chem. Soc., Dalton Trans.* **1996**, 3805–3812.
- (25) Desiraju, G. R. *J. Chem. Soc., Dalton Trans.* **2000**, 3745–3751.
- (26) Brammer, L.; Mareque Rivas, J. C.; Atencio, R.; Fang, S.; Pigge, F. C. *J. Chem. Soc., Dalton Trans.* **2000**, 3855–3867.
- (27) For example, see: (a) Kim, Y.; Verkade, J. G. *Inorg. Chem.* **2003**, *42*, 4262–4264. (b) Chandrasekhar, V.; Nagendran, S.; Bansal, S.; Cordes, A. W.; Vij, A. *Organometallics* **2002**, *21*, 3297–3300. (c) Beatty, A. M. *CrystEngComm* **2001**, *1*, 1–13 and references therein. (d) Qin, Z.; Jennings, M. C.; Puddephatt, R. J. *Inorg. Chem.* **2001**, *40*, 6220–6228. (e) Braga, D.; Greponi, F. *Acc. Chem. Res.* **2000**, *33*, 601–608 and references therein. (f) Gianneschi, N. C.; Tiekink, E. R. T.; Rendina, L. M. *J. Am. Chem. Soc.* **2000**, *122*, 8474–8479. (g) MacDonald, J. C.; Dorrestein, P. C.; Pilley, M. M.; Foote, M. M.; Lundburg, J. L.; Henning, R. W.; Schultz, A. J.; Manson, J. L. *J. Am. Chem. Soc.* **2000**, *122*, 11692–11702. (h) Aakeröy, C. B.; Beatty, A. M.; Leinen, D. S. *Angew. Chem., Int. Ed.* **1999**, *38*, 1815–1819. (i) Sigel, R. K. O.; Freisinger, E.; Metzger, S.; Lippert, B. *J. Am. Chem. Soc.* **1998**, *120*, 12000–12007.
- (28) Prokopuk, N.; Weinert, C. S.; Siska, D. P.; Stern, C. L.; Shriver, D. F. *Angew. Chem., Int. Ed.* **2000**, *39*, 3312–3314.
- (29) Selby, H. D.; Roland, B. K.; Carducci, M. D.; Zheng, Z. *Inorg. Chem.* **2003**, *42*, 1656–1662.
- (30) Roland, B. K.; Selby, H. D.; Cole, J. R.; Zheng, Z. *J. Chem. Soc., Dalton Trans.* **2003**, 4307–4312.

- (31) Ehrlich, G. M.; Warren, C. J.; Vennos, D. A.; Ho, D. M.; Haushalter, R. C.; DiSalvo, F. *J. Inorg. Chem.* **1995**, *34*, 4454–4459.
- (32) Halle, J.-C.; Lelievre, J.; Terrier, F. *Can. J. Chem.* **1996**, *74*, 613–620.
- (33) Chrystiuk, E.; Williams, A. *J. Am. Chem. Soc.* **1987**, *109*, 3040–3046.
- (34) Mayer, J. M.; Testa, B. *Helv. Chim. Acta* **1982**, *65*, 1868–1884.
- (35) Jahagirdar, D. V.; Arbad, B. R.; Kharwadkar, R. M. *Indian J. Chem., Sect. A* **1988**, *27*, 601–605.
- (36) Chebotarev, A. N.; Kachan, S. V. *Russ. J. Phys. Chem.* **1991**, *65*, 360–362.
- (37) Kulig, J.; Lenarcik, B.; Rzepka, M. *Pol. J. Chem.* **1987**, *61*, 59–68.

based ligands to a  $Pd^{2+}$  pincer complex.<sup>38</sup> To our knowledge, this approach has never been applied to binding of ligands to multinuclear metal clusters. Application of the Hammett equation to the binding abilities of this group of ligands to  $W_6S_8$  clusters will add to the body of knowledge about thermodynamics of ligand-exchange reactions involving these clusters.

Here, we report the results of our studies of ligand-exchange reactions involving this family of pyridine-based ligands, including a comparison of binding strengths and synthesis and structural characterization of  $W_6S_8(4\text{-pyridineacetamide})_6$  (**1**) and  $W_6S_8(4\text{-aminopyridine})_6$  (**2**), the first of which crystallizes in a three-dimensional hydrogen-bonded network.

## Experimental Section

**General.** All manipulations were performed with standard air-free techniques in an argon-filled glovebox or using Schlenk equipment, unless otherwise noted. Tetrahydrofuran (THF), diethyl ether ( $Et_2O$ ), and toluene were distilled from sodium benzophenone ketyl before use. Acetonitrile (MeCN), dimethyl sulfoxide (DMSO), and dimethylformamide (DMF) were dried over 4 Å molecular sieves and distilled. Pyridine was dried over 4 Å molecular sieves and then degassed using the freeze-pump-thaw method. Deuterated solvents ( $DMF-d_7$  and  $DMSO-d_6$ ) were purchased from Cambridge Isotopes Laboratory and used as received.  $W_6S_8(n\text{-butylamine})_6$  and  $W_6S_8(tbp)_6$  ( $tbp = 4\text{-tert-butylpyridine}$ ) were synthesized as reported previously.<sup>9,31</sup> The following ligands were purchased commercially and used as received: 4-pyridineacetamide (Alfa Aesar), 4-aminopyridine (Aldrich), 4-hydroxypyridine (Aldrich), isonicotinamide (Aldrich), and isonicotinic acid (Aldrich). The “reaction bomb” referred to below is a custom-made, thick-walled glass vessel equipped with a Teflon valve.

<sup>1</sup>H NMR spectra were collected on Varian Inova 400 and Varian Mercury 300 spectrometers. Spectra were internally referenced against residual protonated solvent peaks ( $\delta 8.03$  for  $DMF-d_7$  and  $\delta 2.50$  for  $DMSO-d_6$ ). Routine spectra were collected with a delay time of  $d1 = 1$  s, whereas a longer delay time of  $d1 = 20$  s was used for quantitative experiments.

Thermogravimetric analyses (TGA) were performed on a TA Instruments TGA Q500 thermoanalyzer using aluminum pans. Samples were heated from room temperature to 550 °C at a rate of 20 °C/min under a flow of nitrogen gas. The gas flow rate at the sample was 60 mL/min, while the balance flow rate was 40 mL/min. Weight loss percentages and onset temperatures were determined using the TA Universal Analysis 2000 software accompanying the instrument.

Powder diffraction experiments were carried out on a Scintag XDS 2000 diffractometer. Elemental analysis was done by Robertson Microлит Laboratories, Madison, NJ.

**Synthesis of  $W_6S_8(4\text{-pyridineacetamide})_6$  (**1**).** In the glovebox, a reaction bomb was charged with  $W_6S_8(n\text{-butylamine})_6$  (35 mg, 0.019 mmol), 4-pyridineacetamide (135 mg, 1.0 mmol, approximately 50 equiv), and DMF (1.5 g) and sealed with a Teflon stopcock. Outside the glovebox, the reaction vessel was heated in an oil bath to 95 °C. The reaction solution turned from greenish-brown to deep red within minutes, and needlelike crystals began to form at the bottom of the bomb. The temperature was held at 95

°C for 2 h and then cooled to room temperature over approximately 6 h. The crystals were collected on a frit, washed with excess THF, and dried in vacuo. The isolated product weighed 29 mg (64% yield). At room temperature, the product was moderately soluble in DMSO and DMF and insoluble in other common organic solvents. <sup>1</sup>H NMR ( $DMSO-d_6$ ):  $\delta 9.06$  (d, *o*-H, 2H,  $J = 6.6$  Hz),  $\delta 8.00$  (s, residual DMF of crystallization),  $\delta 7.63$  (s, amide H, 1H),  $\delta 7.36$  (d, *m*-H, 2H,  $J = 6.6$  Hz),  $\delta 7.08$  (s, amide H, 1H),  $\delta 3.55$  (s, methylene H, 2H),  $\delta 2.59$ ,  $\delta 2.57$  (both d, residual DMF of crystallization). Integration of NMR signals showed that the stoichiometry of this compound was  $W_6S_8(4\text{-pyridineacetamide})_6 \cdot 0.8DMF$ , with an average of 0.8 DMF molecules of crystallization per cluster. Anal. Calcd for  $W_6S_8C_{44.4}H_{53.6}N_{12.8}O_{6.8}$ : C, 24.12; H, 2.38; N, 8.28. Found: C, 23.86; H, 2.42; N, 8.02.

**Synthesis of  $W_6S_8(4\text{-aminopyridine})_6$  (**2**).** A reaction bomb was charged with  $W_6S_8(n\text{-butylamine})_6$  (35 mg, 0.019 mmol), 4-aminopyridine (100 mg, 1.06 mmol, 55 equiv), and DMF (1.875 g). The vessel was heated to 95 °C for 2 h and then cooled to room temperature over 6 h. The mixture turned from greenish-brown to dark red within minutes at elevated temperature. The bomb was inverted twice by hand at the start of heating to ensure dissolution of the starting materials, but the mixture was not stirred constantly. Crystals began to appear while the reaction mixture was still hot, and by the end of the cooling period, many dark, platelike crystals had collected at the bottom of the bomb, leaving behind a light brown solution. The crystals were collected on a frit, washed with THF, and dried in vacuo. The collected product weighed 17.5 mg (42% yield). <sup>1</sup>H NMR ( $DMSO-d_6$ ):  $\delta 8.48$  (m, *o*-H, 2H,  $J = 6.9$  Hz),  $\delta 8.00$  (s, residual DMF of crystallization),  $\delta 6.53$  (s, amine H, 2H), and  $\delta 6.46$  (m, *m*-H, 2H,  $J = 6.9$  Hz). Comparison of the areas of product peaks with peaks from the residual solvent of crystallization showed that an average of 2.4 DMF molecules per cluster remained after drying. Anal. Calcd for  $W_6S_8C_{37.2}H_{52.8}N_{14.4}O_{2.4}$ : C, 21.28; H, 2.53; N, 9.60. Found: C, 21.09; H, 2.31; N, 10.06.

**Reactions of  $W_6S_8$  Clusters with 4-Hydroxypyridine, Isonicotinamide, and Isonicotinic Acid.** Experimental details for syntheses involving  $W_6S_8$  clusters and these pyridine-based ligands are available as Supporting Information.

**Quantitative Studies of Ligand Replacement Reactions.** Stock solutions of  $W_6S_8(tbp)_6$ , pyridine, 4-pyridineacetamide, 4-hydroxypyridine, 4-aminopyridine, and isonicotinamide were prepared in  $DMF-d_7$ . In a typical experimental setup, the  $W_6S_8(tbp)_6$  solution was prepared by transferring 6.7 mg of the cluster solid to a vial containing 5.005 g of solvent. The solution became colored, but the solid did not fully dissolve. After allowing the mixture to equilibrate for approximately one-half an hour, the solution was filtered through a syringe filter, and either 3.0  $\mu$ L of toluene or 1.9 mg of pentamethylbenzene (PMB) was added as an internal standard. A <sup>1</sup>H NMR spectrum of this solution was collected, and the cluster concentration was determined from the internal standard peaks. For each ligand stock solution, approximately 10 mg of the appropriate ligand was weighed in a vial, and approximately 0.3 g of solvent was added to dissolve the ligand. The exact concentration of each solution was calculated. NMR reaction tubes were prepared by first using a 1 mL syringe to transfer 0.70 mL of the cluster stock solution. A 10  $\mu$ L syringe was then used to transfer the volume of ligand stock solution needed to provide 6 equiv of the ligand (approximately 5–8  $\mu$ L for each solution). The tubes were sealed with threaded caps and septa, and the tops were wrapped with Parafilm as an extra barrier against air leakage and solvent loss. <sup>1</sup>H NMR spectra were taken for all five tubes prior to heating. A delay time of  $d1 = 20$  s was used to ensure full relaxation of all protons. The tubes were then heated in a 95 °C oil bath for 3 h,

(38) van Manen, H.-J.; Nakashima, K.; Shinkai, S.; Kooijman, H.; Spek, A. L.; van Veggel, F. C. J. M.; Reinhoudt, D. N. *Eur. J. Chem.* **2000**, 2533–2540.

**Table 2.** Single-Crystal X-ray Refinement Data for Compounds **1** and **2**

	<b>1</b> ·4-pyridineacetamide·DMF	<b>2</b> ·4DMF
chemical formula	W <sub>6</sub> S <sub>8</sub> C <sub>52</sub> N <sub>15</sub> O <sub>8</sub>	W <sub>6</sub> S <sub>8</sub> C <sub>42</sub> H <sub>64</sub> N <sub>16</sub> O <sub>4</sub>
formula weight	2322.25	2156.54
space group	<i>P</i> 2 <sub>1</sub> / <i>c</i>	<i>P</i> 2 <sub>1</sub> / <i>c</i>
<i>a</i> (Å)	16.461(11)	13.8988(5)
<i>b</i> (Å)	33.08(2)	13.2791(5)
<i>c</i> (Å)	13.165(10)	15.6293(6)
$\beta$ (deg)	103.270(15)	108.5410(10)
volume (Å <sup>3</sup> )	6977(9)	2734.88(18)
<i>Z</i> , $\rho$ (g/cm <sup>3</sup> )	4, 2.211	2, 2.619
$\mu$ (mm <sup>-1</sup> )	10.148	12.927
<i>R</i> <sub>1</sub> ( <i>I</i> > 2 $\sigma$ /all) <sup>a</sup>	0.0846/0.1776	0.0360/0.0588
w <i>R</i> <sub>2</sub> ( <i>I</i> > 2 $\sigma$ /all) <sup>b</sup>	0.2128/0.2704	0.0738/0.0809

$$^a R_1 = \sum ||F_o| - |F_c|| / \sum |F_o|. \quad ^b wR_2 = [\sum w(F_o^2 - F_c^2)^2 / \sum w(F_o^2)^2]^{1/2}.$$

and <sup>1</sup>H NMR spectra were obtained again. The reaction mixtures began as orange solutions. After heating, all four had turned some shade of red-brown, and some precipitation had occurred, as evidenced by the formation of a dark solid film around the meniscus of the solution or by the appearance of small amounts of dark, fluffy solids.

**X-ray Structure Determination.** Dark red, needlelike single crystals of W<sub>6</sub>S<sub>8</sub>(4-pyridineacetamide)<sub>6</sub> (**1**) and dark red, platelike single crystals of W<sub>6</sub>S<sub>8</sub>(4-aminopyridine)<sub>6</sub> (**2**) suitable for diffraction experiments were grown as described above. Crystals were mounted on thin plastic loops using polybutene oil and immediately cooled to 173 K in a cold stream of nitrogen. Single-crystal diffraction data were collected on a Bruker SMART<sup>39</sup> system with a CCD detector using Mo K $\alpha$  radiation. The cell parameters were initially determined using more than 50 well-centered reflections. The data were integrated using SAINT<sup>39</sup> software, and empirical absorption corrections were determined and applied using the SADABS<sup>40</sup> program. The space group *P*2<sub>1</sub>/*c* was determined for each crystal on the basis of systematic absences and intensity statistics and was confirmed by the ability to solve the structures.

The structures were solved by direct methods using the SHELX<sup>41</sup> suite. Initial solutions, including positions of heavy atoms, were found using SHELXS, and positions of ligand atoms were determined using SHELXL to perform successive least-squares refinements on *F*<sub>o</sub><sup>2</sup>. For **1**, anisotropic refinement was applied to the W atoms. For **2**, anisotropic refinement was successfully applied to all non-hydrogen atoms, and hydrogen atoms were added using a riding model. Details of the crystal data and refinements are shown in Table 2.

## Results and Discussion

**Synthesis of W<sub>6</sub>S<sub>8</sub>(4-pyridineacetamide)<sub>6</sub> (**1**) and W<sub>6</sub>S<sub>8</sub>(4-aminopyridine)<sub>6</sub> (**2**).** The synthesis of **1** and **2** through ligand substitution on W<sub>6</sub>S<sub>8</sub> proceeded as expected based on our previous experience with cluster ligand-exchange reactions.<sup>10</sup> Because the axial Lewis-basic ligands are rather labile in comparison with the inert W<sub>6</sub>S<sub>8</sub> cluster core, the outer ligands may be exchanged while keeping the core intact. Because of the low solubility of the 4-pyridineacetamide and 4-aminopyridine molecules in solvents such as THF, benzene, and

methylene chloride, DMF was selected as the solvent in which to carry out these reactions. DMSO also dissolves the reactants and products, but heating W<sub>6</sub>S<sub>8</sub> clusters in this solvent has previously been found to lead to decomposition of the cluster compounds.<sup>42</sup> W<sub>6</sub>S<sub>8</sub>(*n*-butylamine)<sub>6</sub> was chosen over W<sub>6</sub>S<sub>8</sub>(*tbp*)<sub>6</sub> as the starting compound for these reactions because of its good solubility in DMF. Monitoring by <sup>1</sup>H NMR spectroscopy showed that both reactions were complete within 2 h. Further heating of the reaction mixture of **1** often led to decomposition of the product, as evidenced by a dark brownish-black coating that formed on the reaction vessel and by low product yields. Synthesis of **1** could also be achieved by using 12–20 equiv of 4-pyridineacetamide, although use of 50 equiv led to more reproducible yields and crystal growth.

<sup>1</sup>H NMR characterization of solutions of **1** and **2** in DMSO-*d*<sub>6</sub> confirmed the attachment of the pyridine-based ligands to W<sub>6</sub>S<sub>8</sub> through the pyridine nitrogen and the effective separation of the products from the excess free ligand present in the reaction solutions. As expected, there is a downfield shift of the ring proton signals ( $\delta$ 8.51 to  $\delta$ 9.06 and  $\delta$ 7.31 to  $\delta$ 7.63) that accompanies binding of the ligand to the tungsten cluster in **1**. A smaller downfield shift ( $\delta$ 3.46 to  $\delta$ 3.55) is observed in the methylene proton signal, and the two amide proton positions are essentially unchanged. In **2**, the ring proton signals are also shifted downfield ( $\delta$ 7.95 to  $\delta$ 8.48 and  $\delta$ 6.44 to  $\delta$ 6.46) upon binding of the ligand to the cluster. There is also a substantial shift ( $\delta$ 5.96 to  $\delta$ 6.53) of the amine proton signal. This large shift could indicate some interaction between metal centers and the ligand amino group, although we expected that the ligand would bind only through the pyridine nitrogen because the NH<sub>2</sub> group in aniline had been previously found not to coordinate to the cluster.<sup>10</sup> In addition, X-ray structural data show that all six ligands bind to the cluster through the pyridine nitrogen (*vide infra*). This large change in the shift of the amino protons upon binding must be due instead to the direct conjugation between the pyridine nitrogen binding site and the amino nitrogen or to changes in the extent of hydrogen bonding experienced by the amino protons.

It was possible to isolate bulk single crystals of **1** and **2** directly from reaction mixtures when the reactions were carried out at high enough concentrations (20 mg of W<sub>6</sub>S<sub>8</sub> cluster/g of DMF). At lower reaction concentrations (e.g., 11 mg of cluster/g of DMF), heating resulted in production of dark red solutions with no visible solid. The pure product **1** could alternatively be isolated by layering it with an equal volume of THF. Over a period of approximately 1 week, a fine, dark red powder precipitated from the solution. <sup>1</sup>H NMR characterization showed that this method effectively separated the product from the large excess of free 4-pyridineacetamide remaining in solution, but powder diffraction revealed that the powder was of poor crystallinity, with very weak diffraction peaks. Several methods, including vapor diffusion, layering, and cooling of saturated solutions, were used in trying to recrystallize this fine powder. These

(39) SMART and SAINT: Data Collection and Processing Software for the SMART system, Bruker Analytical X-ray Instruments Inc., 1995.

(40) Sheldrick, G. M. The computer program SADABS is used by Bruker CCD diffractometers, Institut für Anorganische Chemie der Universität Göttingen, 1996.

(41) Sheldrick, G. M. *SHELXL* Version 5.1, for Bruker Analytical X-ray Instruments Inc., 1997.

(42) Rayburn, L. L. Ph.D. Dissertation, Cornell University, 2001.

**Table 3.**  $^1\text{H}$  NMR Chemical Shifts for Bound and Unbound Pyridine-Based Ligands

ligand	$\delta$ (ortho protons)		$\delta$ (meta protons)	
	bound	unbound	bound	unbound
4- <i>tert</i> -butylpyridine	9.26	8.51	7.57	7.42
pyridine <sup>a,b</sup>		8.61		7.35
isonicotinamide	9.51	8.76	7.95	7.88
4-hydroxypyridine	9.02	7.84	6.90	6.28
4-aminopyridine	8.72	8.04	6.77	6.58
4-pyridineacetamide	9.26	8.51	7.46	7.35

<sup>a</sup> Shift for para proton of unbound pyridine:  $\delta 7.82$ . <sup>b</sup> Shifts for bound pyridine not available because of insolubility of pyridine-ligated clusters in  $\text{DMF-}d_7$ .

methods led either to no precipitation or to formation of extremely small, clumped needles not suitable for single-crystal diffraction experiments. Thus, crystallization of **1** directly from concentrated reaction mixtures was found to be the only means of obtaining diffraction-quality crystals.

**Comparison of Ligand Binding Abilities.** Quantitative  $^1\text{H}$  NMR experiments were used to compare the abilities of ligands in this family to compete with *tbp* in coordinating the  $W_6S_8$  cluster. The general approach used was that developed previously,<sup>42</sup> but some modifications were made to accommodate this system of ligands. No solvent was found that is capable of dissolving the  $W_6S_8$  cluster as well as all of the ligands pictured in Table 1.  $\text{DMF-}d_7$  was selected as the solvent that was able to dissolve the most species, although isonicotinic acid had to be excluded from the study because it is not sufficiently soluble in DMF.

$^1\text{H}$  NMR spectra were taken of each reaction tube prior to heating and again after 3 h at 95 °C. Peak assignments for free and bound ligands were made on the basis of spectra that had been collected for pure ligands and clusters in  $\text{DMF-}d_7$ . Chemical shifts for the pyridine ring protons in these species are tabulated in Table 3. The spectra in  $\text{DMF-}d_7$  are descriptively the same as those collected in  $\text{DMSO-}d_6$  and reported in the synthesis section, but there are minor differences in chemical shifts. For pyridine, no shifts for the bound ligand are reported because clusters ligated with pyridine are not soluble in  $\text{DMF-}d_7$ .<sup>31</sup>

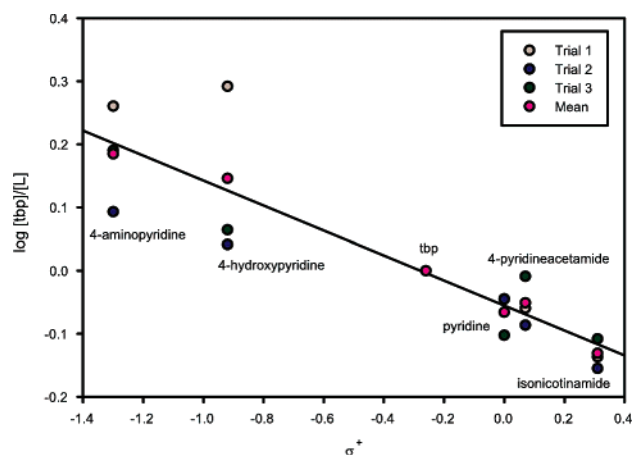
For each trial,  $^1\text{H}$  NMR spectra were obtained prior to heating, and integrations of peaks belonging to bound *tbp* and to the new free ligand in each tube were used to confirm the initial ratio of approximately six bound *tbp* ligands to six competing ligands. After heating, spectra were taken again, and the peak integrations for the remaining unbound competing ligand and for free *tbp* liberated through the reaction were used to calculate the ratio  $[\text{tbp}]/[\text{L}]$ . Because calculation of equilibrium or stability constants was beyond the scope of these experiments, this ratio was used as an indicator of the extent of replacement of *tbp* by the competing ligand L. This approach also allows us to focus only on free ligand peaks, which was desirable because peaks from bound ligands were often broad due to the mixture of isomers present or very small due to lack of solubility of the substituted product.

The  $[\text{tbp}]/[\text{L}]$  ratios found in all three trials are shown in Table 4. The uncertainties reported along with the mean

**Table 4.** Free Ligand Ratios after Heating of Ligand-Exchange Reactions

competing ligand (L)	$\sigma^+$	$[\text{tbp}]/[\text{L}]$ ratio			
		trial 1	trial 2	trial 3	mean <sup>a</sup>
pyridine	0.00	0.90	0.90	0.79	$0.86 \pm 0.064$
isonicotinamide	0.31	0.73	0.70	0.78	$0.74 \pm 0.040$
4-pyridineacetamide	0.07	0.87	0.82	0.98	$0.89 \pm 0.081$
4-hydroxypyridine	-0.92	1.96	1.10	1.16	$1.40 \pm 0.48$
4-aminopyridine	-1.3	1.82	1.24	1.55	$1.53 \pm 0.29$
4- <i>tert</i> -butylpyridine	-0.26	1.00 <sup>b</sup>	1.00 <sup>b</sup>	1.00 <sup>b</sup>	1.00 <sup>b</sup>

<sup>a</sup> Uncertainty given is the calculated standard deviation for the set of data. <sup>b</sup> Ideal value for competition of *tbp* with itself or with another ligand L of identical binding ability.

**Figure 1.** Hammett plot for extent of replacement for reactions of  $W_6S_8(\text{tbp})_6$  with competing pyridine-based ligands (L). The line shown was found through a least-squares fit of the mean data points.

values are the standard deviations calculated for the three trials. A ligand with binding ability exactly equal to that of *tbp* would be expected to result in a reaction with  $[\text{tbp}]/[\text{L}] = 1$ . As may be seen, there was considerable variation in the data from trial to trial, particularly for 4-hydroxypyridine and 4-aminopyridine. The results appear to be very sensitive to details of reaction conditions, including the exact time and temperature of heating. Qualitatively, the  $[\text{tbp}]/[\text{L}]$  ratios reported in Table 4 follow the same order as the Hammett substituent constants  $\sigma^+$  for the pyridine substituents. This relationship may also be seen graphically in Figure 1. Although there is appreciable spread in the data points, the plot shows that extent of binding increases with decreasing  $\sigma^+$  and that the mean data points fall near a best-fit line with  $r^2 = 0.984$ . The dual parameter  $\sigma^+$  was found to better fit the behavior of the ligands than the single parameter  $\sigma$ , showing that the resonance between substituent groups and the pyridine nitrogen is important in these coordination reactions. The dual  $\sigma^+$  parameter was also used in a previous study of binding of pyridine-based ligands to a  $\text{Pd}^{2+}$  complex.<sup>38</sup> This set of experiments shows that Hammett substituent constants can be a good qualitative predictor of binding ability of pyridine-based ligands. Notably, the Hammett  $\sigma$  parameter is a better predictor of ligand binding strength for this family of ligands than is  $\text{p}K_a$ . The negative value ( $-0.20$ ) of the slope of the best-fit line is in contrast with the positive slopes found for binding of pyridine-based ligands to late transition metals where  $\pi$  back-bonding is

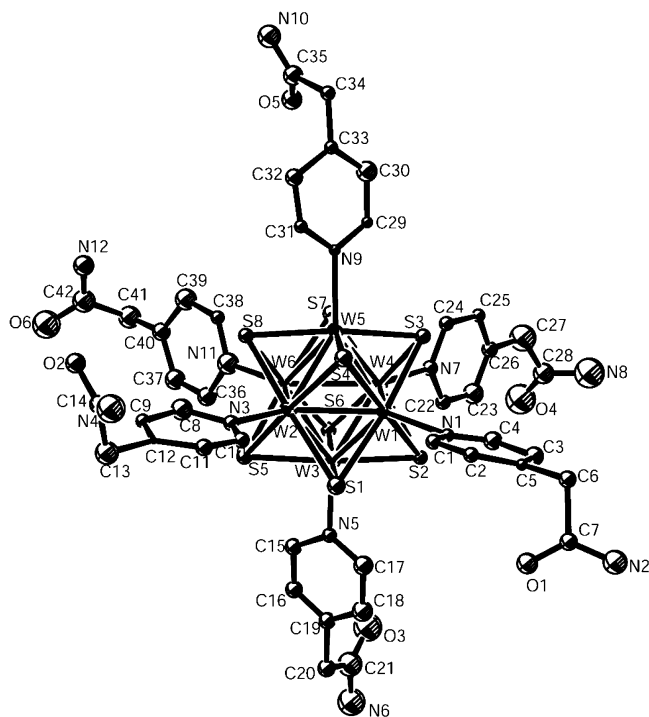


**Figure 2.** ORTEP representation of molecular unit of  $W_6S_8(4\text{-pyridineacetamide})_6$  (**1**) drawn at 40% probability.

significant.<sup>37</sup> This shows that  $\sigma$  donation dominates in the binding of these ligands to the  $W_6S_8$  cluster.

**Molecular and Supramolecular Structures.** Single-crystal X-ray diffraction was used to find structures for  $W_6S_8(4\text{-pyridineacetamide})_6$  (**1**) and  $W_6S_8(4\text{-aminopyridine})_6$  (**2**). ORTEP<sup>43</sup> representations of the molecular units of both are shown in Figures 2 and 3, respectively. The asymmetric unit of **1** contains one  $W_6S_8$  cluster with six bound ligands in addition to a free 4-pyridineacetamide ligand and one DMF molecule. The refinement residuals,  $R_1$  and  $wR_2$ , were 0.0846 (for  $I > 2\sigma$ ) and 0.2128 (for  $I > 2\sigma$ ), respectively. These are somewhat larger than the typical  $R_1$  and  $wR_2$  values of 0.04 and 0.09, respectively, found in previous refinements of several  $W_6S_8$  compounds.<sup>10</sup> One reason that the values for **1** are not lower is that the fine, needlelike crystals grown in reaction mixtures exhibit a degree of mosaicity. Peak profiles viewed using the SMART software showed some broadness and asymmetry in peak shapes. Disorder was also observed in the position of the DMF solvent molecule. Several crystals from different reaction batches were examined and were all found to display this characteristic. Due to the broadness and asymmetry, integration of peak intensities for use in structure refinement is likely to produce larger-than-normal errors that would be reflected in larger refinement residuals. In addition, accurate absorption corrections are challenging for needlelike crystals. As discussed above, alternative crystal growth methods did not lead to diffraction-quality crystals. Because of the inherent disorder in this system and the needlelike habit of the crystals, some uncertainty remains in the structure solution. The structure solution shown here represents the maximum

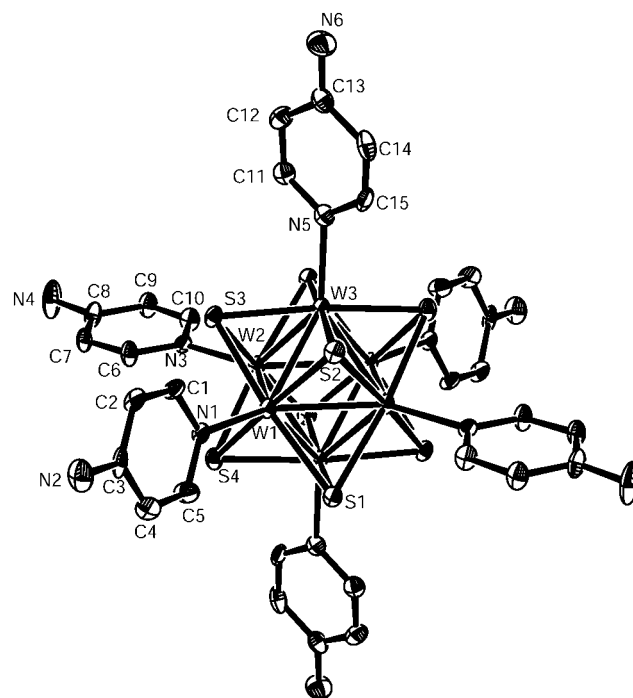


**Figure 3.** ORTEP representation of molecular unit of  $W_6S_8(4\text{-aminopyridine})_6$  (**2**) with thermal ellipsoids drawn at 50% probability.

information that can be derived from the data that are available.

The asymmetric unit for **2** contains a  $W_3S_4$  cluster fragment and three bound ligands in addition to two DMF molecules. The refinement residuals,  $R_1$  and  $wR_2$ , were 0.0360 (for  $I > 2\sigma$ ) and 0.0738 (for  $I > 2\sigma$ ), respectively. Some disorder was noted in the solvent molecules in **2**. For each of the two DMF molecules in the asymmetric unit, only one of the methyl carbon atoms could be easily resolved in the Fourier difference map.

Selected averages and ranges for bond lengths and angles in **1** and **2** are given in Table 5 in comparison with those known for  $W_6S_8(4\text{-tert-butylpyridine})_6$ .<sup>31</sup> The  $W_6$  octahedron is regular for all three compounds, as indicated both by  $W-W$  distances and by  $W-W-W$  bond angles. The average  $W-W$  distance in **1** is 2.656(17) Å, slightly shorter than the value of 2.662(6) Å found for  $W_6S_8(4\text{-tert-butylpyridine})_6$ , whereas the average distance in **2** is slightly longer at 2.667(7) Å. For these three compounds, there appears to be a relationship between ligand binding strength and mean  $W-W$  distance. As discussed above, <sup>1</sup>H NMR studies showed that 4-aminopyridine is the most strongly bound of these three ligands, and the structure of **2** shows the largest mean  $W-W$  distance. The same general trend was observed in the larger group of N- and P-ligated clusters synthesized previously and was attributed to the need to maintain a constant valence sum for tungsten.<sup>10</sup>

The average  $W-S$  distances are in good agreement among **1**, **2**, and  $W_6S_8(\text{tbp})_6$ , although the value of 2.456(13) Å for **1** is slightly smaller than the values of 2.463(7) and 2.461(5) Å in **2** and  $W_6S_8(\text{tbp})_6$ , respectively. The average  $W-L$  distance in  $W_6S_8$  clusters has previously been examined as an indication of the strength of ligand coordination, and this

(43) Farrugia, L. J. *J. Appl. Crystallogr.* **1997**, *30*, 565.

**Table 5.** Selected Bond Lengths (Å) and Angles (deg) for Compounds **1** and **2**

	<b>1</b>	<b>2</b>	$W_6S_8(\text{tbp})_6$ <sup>a</sup>
W–W mean	2.656(17)	2.667(7)	2.662(6)
W–W range	2.626(3)–2.683(3)	2.6588(4)–2.6785(4)	2.656(1)–2.667(1)
W–N mean	2.24(1)	2.245(11)	2.257(8)
W–N range	2.23(3)–2.25(3)	2.233(6)–2.255(5)	
W–S mean	2.456(13)	2.463(7)	2.461(5)
W–S range	2.423(8)–2.481(9)	2.455(2)–2.477(2)	2.458(2)–2.469(2)
W–W–W mean <sup>b</sup>	89.99(51)		
W–W–W range <sup>b</sup>	89.23(6)–90.63(7)	89.74(1)–90.27(1)	89.3(1)–90.3(1)
W–W–W range <sup>c</sup>	58.82(6)–60.96(6)	59.73(1)–60.35(1)	59.9(1)–60.3(1)

<sup>a</sup> From ref 31. <sup>b</sup> Within equatorial squares. The mean W–W–W angle is constrained to 90° if the cluster is centered on an inversion center. <sup>c</sup> Within triangular faces. The mean W–W–W angle is automatically 60° by geometry.

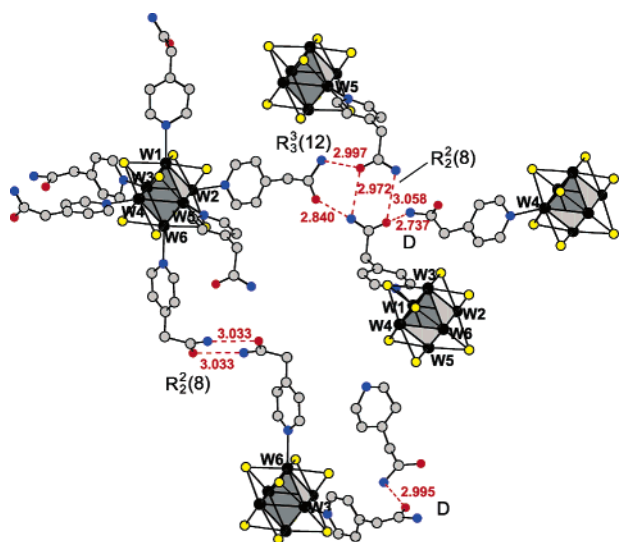


**Figure 4.** Local hydrogen-bonding environment in **1**. Distances between nitrogen (blue) and oxygen (red) are given in angstroms. The notations  $R_2^2(8)$ ,  $R_3^3(12)$ , and D refer to the graph set analysis of Etter (refs 22, 47, 48).

is again of interest for this group of compounds. The range of distances observed here (2.24(1)–2.57(8) Å) is smaller than the variation observed earlier (2.160(10)–2.570(12) Å),<sup>10</sup> and values for **1** and **2** are within experimental uncertainties of one another. This is due to the similar binding strengths of the pyridine-based ligands as compared to the broader range of binding abilities seen previously for a variety of P- and N-based ligands.

The most interesting features of **1** and **2** arise when considering not their molecular structures but their supra-molecular structures. With the six ligands coordinated to  $W_6S_8$  through the pyridine nitrogens in each compound, the amine and amide functionalities are available for participation in intermolecular interactions with molecules of crystallization and with other cluster molecules. This is especially interesting in compound **1**, in which hydrogen-bonding interactions create a three-dimensional network of clusters. All six of the pyridineacetamide ligands participate in hydrogen bonding, as shown in Figure 4. Because of the presence of the very electron-dense tungsten clusters, we would not expect to be able to see hydrogen atoms in the Fourier difference map for this compound, and N···O distances were used to identify hydrogen-bonding interactions. This method was used previously for a hydrogen-bonded structure containing electron-dense  $Mo_6Cl_8^{4+}$  clus-

ters.<sup>28</sup> N···O distances observed in this structure fall in the range of 2.737–3.058 Å, consistent with the moderately strong hydrogen bonding found in amides.<sup>44,45</sup> Taylor's survey<sup>46</sup> of 1509 N–H···O=C hydrogen bonds reported in the Cambridge Structural Database showed a mean N···O distance of 2.878 Å, with a standard deviation of 0.122 Å. The N···O distances found for **1** are all within 1.5 standard deviations of the mean in this distribution.

Three different hydrogen-bonding motifs are observed in this structure. In describing these interactions, it is useful to number the ligands as ligand 1–ligand 6, with the number corresponding to the tungsten atom with which each ligand is associated. Ligand 6 on each cluster is involved in a pairwise, self-complementary interaction which may be described with the very common  $R_2^2(8)$  graph set, in the notation of Etter.<sup>22,47,48</sup> This hydrogen-bonding motif is very common in structures involving organic molecules.<sup>48</sup> Ligand 3 forms a hydrogen bond with the free 4-pyridineacetamide molecule (denoted D in graph set notation) and with a solvent molecule, which is not shown. Ligands 1, 2, 4, and 5 participate in a complicated, tetrameric interaction. The amide nitrogen of ligand 1 is associated with the carbonyl oxygens of both ligands 2 and 5, presumably by involving both of its amide protons. The carbonyl oxygens of ligands 1 and 5 are also each involved in two interactions, acting as acceptors toward two different nitrogen atoms. The ability of both amide nitrogen and carbonyl oxygen atoms to participate in two hydrogen-bonding interactions has been documented,<sup>46</sup> so the observed structure is not surprising. This complicated interaction contains an  $R_2^2(8)$  motif as well as a larger ring that may be denoted as  $R_3^3(12)$ . Notably, although one ligand does interact with the DMF solvent molecule, the solvent does not play a significant role in the structure. This is particularly fortuitous because hydrogen-bonding solvents such as DMF and DMSO have sometimes been found to disrupt hydrogen-bonding networks when used to grow crystals.<sup>27d</sup>

The three-dimensional network formed by these interactions may be pictured by first considering a two-dimensional

- (44) Leiserowitz, L.; Tuval, M. *Acta Crystallogr.* **1978**, *B34*, 1230–1247.  
 (45) Weinstein, S.; Leiserowitz, L. *Acta Crystallogr.* **1980**, *B36*, 1406–1418.  
 (46) Taylor, R.; Kennard, O.; Versichel, W. *Acta Crystallogr.* **1984**, *B40*, 280–288.  
 (47) Etter, M. C.; MacDonald, J. C.; Bernstein, J. *Acta Crystallogr.* **1990**, *B46*, 256–262.  
 (48) Bernstein, J.; Davis, R. E.; Shimon, L.; Chang, N.-L. *Angew. Chem., Int. Ed. Engl.* **1995**, *34*, 1555–1573.

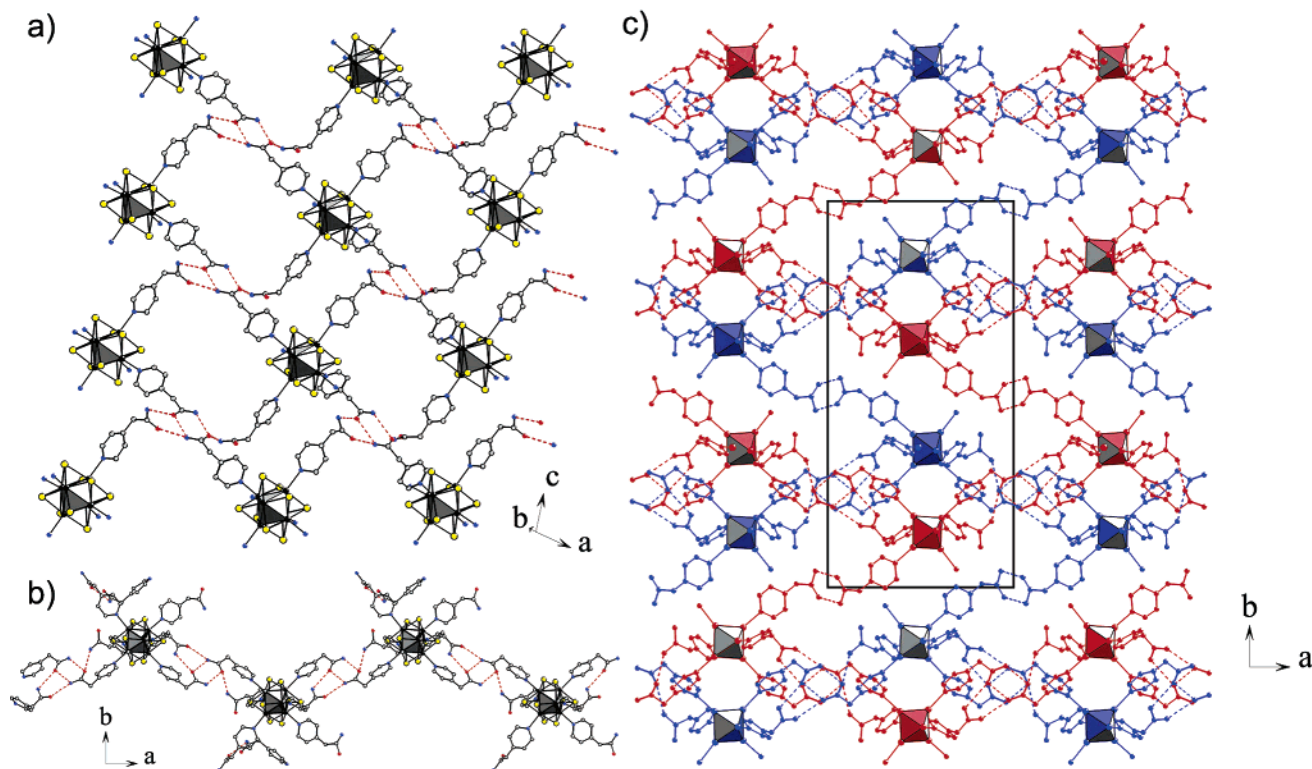


**Figure 5.** (a) View of two-dimensional sheet in **1** approximately along the *b*-axis. Color scheme: W(black), S(yellow), C(gray), N(blue), O(red). (b) View of two-dimensional sheet along the *c*-axis, showing zigzag appearance. (c) Three-dimensional hydrogen-bonded network formed in **1**. Two equivalent interpenetrating nets are shown in contrasting colors. For clarity, solvent molecules and free ligand of crystallization, along with ligand 3, have been omitted, and  $W_6S_8$  clusters are shown as uncapped octahedra.

sheet parallel to the (0 1 0) plane formed through the interactions of ligands 1, 2, 4, and 5 (Figure 5a). When viewed along the *c*-direction (Figure 5b), the corrugated sheets appear as zigzag cross-sections. A view of the entire network, with ligand 3 and the free ligand molecule omitted for clarity, is shown in Figure 5c. In filling the unit cell, the two-dimensional zigzag sheets occur in interpenetrating pairs, or double layers. The double layers are then further connected with one another through the pairwise interactions of ligand 6. Each cluster is located on a general position in the unit cell. Within the double layer, the two sheets are related to one another through a *c*-glide perpendicular to *b*. The two double layers in the unit cell are related to one another via a screw axis in the *b*-direction. The channels seen among clusters in Figure 5c are occupied in part by the free ligand molecule and by ligand 3. Solvent molecules are also located in these channels.

The structure of the hydrogen-bonded network formed in compound **1** could not have been anticipated. It is the first hydrogen-bonded network based on  $W_6S_8$  clusters and only the second 3-D hydrogen-bonded network formed from octahedral metal clusters. The ability of the amide group to act as both a donor and an acceptor for hydrogen bonding may have led one to expect a structure with more pairwise interactions. These pairwise interactions are seen throughout hydrogen-bonded structures formed from  $Re_6Se_8^{2+}$  clusters.<sup>29,30</sup> However, structure **1** differs from these architectures in two important ways. First, the 4-pyridineacetamide ligand is longer and more flexible than the ligands used with  $Re_6Se_8^{2+}$ . Second, and perhaps more importantly, compound

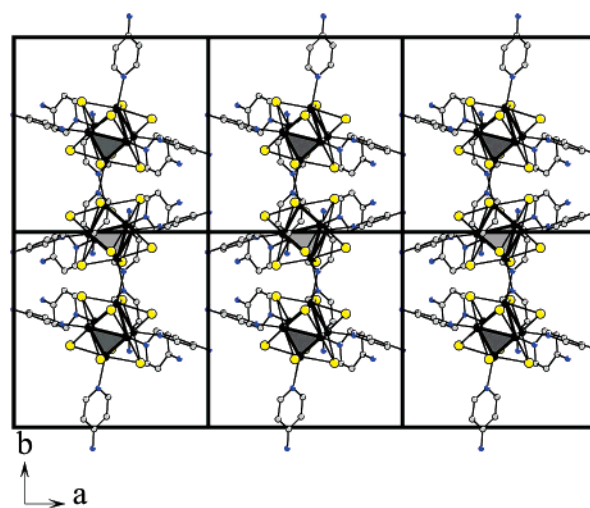


**Figure 6.** Structure of  $W_6S_8(4\text{-aminopyridine})_6$  viewed along the *c*-direction. Hydrogen atoms and solvent molecules have been omitted for clarity. Color scheme: W(black), S(yellow), C(gray), N(blue).

**1** does not contain counterions that help to fill space. The structure that forms from **1** uses the ligands themselves for space-filling and accommodates the length and relative flexibility of the 4-pyridineacetamide molecule.

A view of the structure of **2** along the *c*-direction is shown in Figure 6. Solvent molecules, omitted from this picture, occupy the channels formed among clusters. The unbound amino groups are able to act as hydrogen-bond donors but not as acceptors. This behavior for  $R-NH_2$  groups has been documented before<sup>49</sup> and is consistent with observation of the strong binding ability of 4-aminopyridine toward the



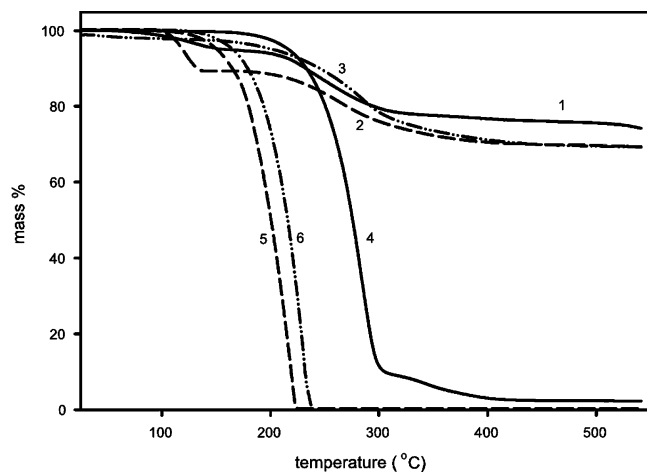


**Figure 7.** TGA traces for compounds **1**, **2**, and **3** and for free 4-pyridine-acetamide (**4**), 4-aminopyridine (**5**), and isonicotinamide (**6**) ligands.

$W_6S_8$  cluster. The enhanced binding ability of this ligand as compared to pyridine is due to the electron-donating character of the amino group, meaning that the amino lone pair has significant delocalization with the pyridine ring. This makes it less accessible for interaction with hydrogen atoms on other molecules. In the structure of **2**, the amino groups on four of the ligands are involved in hydrogen-bonding interactions with the DMF molecules of crystallization, as indicated by  $N\cdots O$  distances of 2.99 and 2.97 Å between amine nitrogens and DMF carbonyl oxygens. However, no hydrogen bonding is observed among ligands coordinated to different clusters, and an extended network does not result.

While no cluster–cluster interactions arise from hydrogen bonding in **2**, there is some evidence of possible intercluster  $\pi$ – $\pi$  interactions. Pairs of ligands on neighboring clusters are parallel to one another when viewed down the  $c$ -axis as in Figure 6. The closest C–C contact between rings on adjacent clusters is 3.19 Å, within the range found for  $\pi$ – $\pi$  stacking in Janiak's survey of the Cambridge Structure Database.<sup>50</sup> The centroid–centroid distance of 4.97 Å is, however, considerably longer than is usually observed for stacking of pyridine rings coordinated to metal centers. The pairs of rings in **2** are parallel to one another but have significant lateral displacement away from a face-to-face orientation. Although at least some degree of lateral displacement is very common in complexes coordinated with pyridine rings, overlap by at least one edge of the pyridine rings is usually seen.<sup>50</sup> Based on the large centroid–centroid distance and lateral displacement observed here, we conclude that any  $\pi$ – $\pi$  interaction is very weak.

**Thermogravimetric Analysis.** TGA experiments were performed on several-milligram samples of **1**, **2**, and  $W_6S_8(\text{isonicotinamide})_{5.5}(\textit{n}\text{-butylamine})_{0.5}$  (**3**) and on the corresponding free ligands, and the resulting traces are shown in Figure 7. Because the onset temperature  $T_d$  of ligand loss for cluster compounds may be used as an indicator of the ease of deligation, TGA measurements were undertaken to

learn how the ligands studied here fit into the hierarchy of ligand binding strengths established earlier for a group of N- and P-based ligands.<sup>10</sup>

The trace for each cluster compound shows two weight-loss steps. The first, at or below approximately 100 °C, represents loss of solvent molecules of crystallization. The second step for each complex corresponds to loss of the ligand molecules and is of interest in assessing the ligand binding strength. Onset temperatures of  $T_d = 218$ , 225, and 232 °C were found for the second step for compounds **1**, **2**, and **3**, respectively. The percent weight loss measured in each case was somewhat less than was predicted for loss of six ligands (for example, an observation of 20.1% versus a predicted 25.5% loss for **2**). This is consistent with findings for other  $W_6S_8$  cluster complexes because pyrolytic processes at high temperatures, perhaps catalyzed by the metal cluster, appear to lead to production of nonvolatile organic material.<sup>42</sup>

The onset temperatures for ligand loss found for compounds **1**, **2**, and **3** are all higher than  $T_d = 190$  °C found earlier for  $W_6S_8(\text{tbp})_6$  and in the range of  $T_d = 220$  °C found for a more strongly bound  $W_6S_8(\textit{n}\text{-butylphosphine})_6$  complex.<sup>10</sup> This would suggest that 4-pyridineacetamide, 4-aminopyridine, and isonicotinamide are all stronger ligands than *tbp*, which is in contradiction with NMR results. In particular,  $T_d$  is surprisingly high for **3**, which was found by NMR studies to be the most weakly bound of these three complexes. However, the ligands examined here are much more involatile than many of the ligands examined previously, largely because of their ability to form intermolecular hydrogen bonds. Indeed, examination of the traces for the free ligands shows that the temperatures at which these species evaporate or sublime are not much below the onset temperatures for weight loss measured for the cluster complexes. Therefore, the  $T_d$ 's measured for the cluster products may be deceptively high because of the involatility of the ligands themselves.

## Conclusions

We have reported here on exploration of ligand-exchange reactions involving  $W_6S_8$  clusters and a family of pyridine-based ligands. These ligands were chosen because they are substituted with moieties with the potential to participate in hydrogen-bonding interactions. The experimental study of these ligands has resulted in the synthesis of three new compounds, two of which were isolated in the form of single crystals. Quantitative  $^1\text{H}$  NMR spectroscopy and TGA have been used to compare the binding abilities of the ligands with one another and with ligands previously used with  $W_6S_8$  clusters. A Hammett plot was constructed on the basis of the  $^1\text{H}$  NMR experiments and shows that substituent constants are useful as qualitative predictors of ligand binding abilities. The results reiterate the importance of  $\sigma$  donation for ligand interactions with these early transition metal clusters.  $W_6S_8(4\text{-pyridineacetamide})_6$  (**1**) and  $W_6S_8(4\text{-aminopyridine})_6$  (**2**) have been isolated as single crystals and characterized by X-ray diffraction. The former compound is of particular interest because it crystallizes to form a three-dimensional network linked through hydrogen bonding. The

(49) Llamas Saiz, A. L.; Foces-Foces, C. *J. Mol. Struct.* **1990**, *238*, 367–382.

(50) Janiak, C. *J. Chem. Soc., Dalton Trans.* **2000**, 3885–3896.

hydrogen-bonding interactions that are observed are consistent with distances and motifs reported in the literature for amide–amide hydrogen bonding and include pairwise interactions as well as more complicated tetrameric associations. This compound represents the first hydrogen-bonded network based on  $W_6S_8$  clusters and only the second 3-D hydrogen-bonded network formed from group 6 metal clusters. This is particularly interesting because it demonstrates that ordering of crystalline assemblies of transition metal species through hydrogen bonding is possible even in the absence of stronger ionic interactions engendered by charged clusters and the space-filling advantages provided by their counterions.

**Acknowledgment.** This work was supported by a grant from the Department of Energy (DE-FG02-87ER45298). C.M.O. thanks the National Science Foundation for a Graduate Research Fellowship and Graduate Teaching Fellowship (DUE-0231913 and -9979516). This work also made use of the Polymer Characterization Facility of the Cornell

Center for Materials Research (CCMR) with support from the National Science Foundation Materials Research Science and Engineering Centers (MRSEC) program (DMR-0079992). S.P.'s work was also supported by the CCMR with funding from the Research Experience for Undergraduates program (DMR-0097494). We acknowledge Dr. Emil Lobkovsky for assistance with single-crystal X-ray diffraction experiments and Professor Barry Carpenter for useful discussions.

**Supporting Information Available:** X-ray crystallographic files in CIF format, including experimental and refinement conditions, lists of atomic positions, anisotropic thermal parameters, and tables of bond lengths and angles, for the structure determinations of  $W_6S_8(4\text{-pyridineacetamide})_6$  and  $W_6S_8(4\text{-aminopyridine})_6$ ; experimental details and results for reactions between  $W_6S_8$  clusters and isonicotinamide, 4-hydroxypyridine, and isonicotinic acid. This material is available free of charge via the Internet at <http://www.pubs.acs.org>.

IC0487225